# Changes in the Medial and Lateral Gastrocnemius Fiber Architecture with Age.

Yanjie Xue[1], Usha Sinha[1], Vadim Malis[1], Robert Csapo[2], and Shantanu Sinha[2]

*[1]Physics, SDSU, San Diego, CA, United States, [2]Radiology, UCSD, San Diego, CA, United States*

**Target Audience:** MSK radiologists (focus on aging, sarcopenia), Image Processing Researchers (focus on fiber tracking).

**Purpose:** Age related changes in muscle alter fiber architecture (fiber lengths and pennation angles). Diffusion tensor imaging (DTI) allows the mapping of fiber architecture; this study investigates age related changes in fiber architecture of the medial and lateral gastrocnemius using DTI.

**Methods:** Five young (32 ± 7 yrs) and five senior (83 ± 3 yrs) Japanese women were recruited with informed consent; participants were free of internal or orthopedic disease. DWI were acquired on a 3 T GE scanner using a fat suppressed single shot EPI sequence without dual 180º pulses. Thirty-two non-collinear gradient directions with a b-factor of 400s/mm$^2$ were used; imaging parameters were (TE)/ (TR): 49 ms/4000 ms, 4averages. The FOV, slice thickness/gap, and matrix were 240 × 240 mm2, 5 mm/0 mm, and 80 × 80 respectively. A custom built coil with a large field of view was used to image approximately 22 cm of the lower leg without moving the subject or coil; the intent was to cover the medial and lateral gastrocnemius muscles from their origin to insertion in a single acquisition. Diffusion weighted image volumes were corrected for eddy current, motion and susceptibility related artifacts, smoothed and masked with the muscle volume of interest: MG or LG. Fiber tracking was performed using DTIStudio (https://www.dtistudio.org/) on the (MG or LG) masked tensor volumes. The stopping criteria for the fiber tracking algorithm were: FA < 0.15 and an angle change > 20$^o$ between successive. ROIs (1 pixel wide) were selected on coronal (reformatted) eigenvector images near the deep aponeurosis at distal and middle locations to extract fibers passing through these ROIs. Several fibers pass through each ROI due to the 'brute-force' nature of the fiber tracking algorithm. Fiber coordinates for each fiber were saved to calculate pennation angles and fiber lengths. The surfaces corresponding to the deep and superficial aponeuroses were automatically identified from the masks. The pennation angle was calculated at the deep/superficial aponeuroses as follows: the closest point on the deep aponeurosis surface to the start point of the fiber was identified. A3x3 neighborhood on the aponeurosis surface near the intersection point was fit to a 3rd order polynomial. The normal to this surface was calculated and the pennation angle was calculated as: (90$^0$-angle between the surface normal and the line joining a point on the fiber to the surface intersection point). Pennation angles were calculated for the fiber start and end points with respect to both aponeuroses; this can provide information on fiber curvature as well as the relative orientations of the distal/superficial aponeuroses. Several automated checks were incorporated into this algorithm to ensure the integrity of the fibers including (i) exclusion of fibers that tracked entirely along the aponeursis (ii) exclusion of fibers that terminated > 3 voxels from the superficial aponeurosis, and (iii) trimming points on the fibers where the fibers ran parallel to the aponeuroses at either surface.

**Results:** Fig. 1a,b,c,d show the medial gastrocnemius fibers from a young and old subject respectively: similar fiber tracts were found in the other subjects. It was difficult to track fibers at the proximal end primarily from the larger geometric distortions at this level and possibly other artifacts arising from ghost artifacts as well as well as mask mismatches (as the muscle tapers toward the proximal end) mismapping. Fig. 1e,f,g,h shows the lateral gastrocnemius fibers tracked from a young and old subject respectively. Table 1 is a summary of the fiber length and pennation angle changes for fibers through ROIs placed in the distal and middle medial and lateral gastrocnemius in the junior and senior subjects. In the MG, a 41% and 17% decrease in length in the older cohort compared to the younger cohort was seen in the distal and middle region respectively; this difference was significant in the distal region (color coded). Fibers were also longer in the distal compared to the middle in the young (43%) and in the old (19%) and the regional difference was significant in both age groups. Three angles were measured for each fiber: d-d: the angle of the deep end of the fiber to the deep aponeurosis surface, s-s: the angle of the superficial end of the fiber to the superficial aponeurosis surface, and s-d: the angle of the superficial end of the fiber to the deep aponeurosis surface. Summarizing the pennation angle findings in the MG, the pennation angle (d-d) was larger in the young compared to the old cohort and larger for fibers originating in the middle compared to the distal region. Significant differences were found in the superficial pennation angles between the young and old cohorts; however the superficial pennation angle was larger in the older cohort. Similar differences among young and old were also present in the superficial-deep (s-d) angles which was significant in the distal region. Regional differences were significant in both age cohorts with angles increasing from distal to middle regions. Comparing the pennation angles (d-d, s-s and s-d), differences were seen between each pair in both the young and old subjects, these differences were significant in the young cohort. In the LG, findings were qualitatively similar to that found in the MG (longer fibers, larger pennation angles at the deep aponeurosis in the younger cohort, and longer fibers, lower pennation angles distal compared to medial origin fibers ). However, the differences were all smaller and significant difference was found only in the superficial pennation angle between young and old.

**Table 1 [length in mm, yellow p<0.05, blue p<0.1]**

| Medial Gastrocnemius | | | |
|---|---|---|---|
| | | Young (Y) | Old (O) |
| Length | Distal(D) | 67.060 | 39.675 |
| | Middle(M) | 38.292 | 31.987 |
| | %diff(D: Y-O) | 40.837 | |
| | %diff(M: Y-O) | 16.465 | |
| | %diff(Y: D-M) | 42.900 | |
| | %diff(O: D-M) | 19.378 | |
| D/D-PA | Distal | 19.422 | 17.786 |
| | Middle | 36.478 | 24.851 |
| | %diff(D: Y-O) | 8.424 | |
| | %diff(M: Y-O) | 31.873 | |
| | %diff(Y: D-M) | -87.816 | |
| | %diff(O: D-M) | -39.723 | |
| S/S-PA | Distal | 12.481 | 24.631 |
| | Middle | 16.330 | 32.144 |
| | %diff(D: Y-O) | -97.349 | |
| | %diff(M: Y-O) | -96.843 | |
| | %diff(Y: D-M) | -30.840 | |
| | %diff(O: D-M) | -30.504 | |
| S/D-PA | Distal | 21.018 | 28.007 |
| | Middle | 28.841 | 33.266 |
| | %diff(D: Y-O) | -33.256 | |
| | %diff(M: Y-O) | -15.343 | |
| | %diff(Y: D-M) | -37.223 | |
| | %diff(O: D-M) | -15.343 | |
| distal | %diff dd-ss | 35.739 | -38.484 |
| middle | %diff dd-ss | 55.233 | -33.860 |
| distal | %diff ss-dd | -68.398 | -13.707 |
| middle | %diff ss-dd | -76.614 | -3.489 |

| Lateral Gastrocnemius | | | |
|---|---|---|---|
| | | Young (Y) | Old (O) |
| Length | Distal(D) | 56.534 | 41.129 |
| | Middle(M) | 37.841 | 41.657 |
| | %diff(D: Y-O) | 27.249 | |
| | %diff(M: Y-O) | -10.083 | |
| | %diff(Y: D-M) | 33.065 | |
| | %diff(O: D-M) | -1.282 | |
| D/D-PA | Distal | 17.160 | 14.813 |
| | Middle | 20.337 | 14.803 |
| | %diff(D: Y-O) | 13.677 | |
| | %diff(M: Y-O) | 27.212 | |
| | %diff(Y: D-M) | -18.515 | |
| | %diff(O: D-M) | 0.067 | |
| S/S-PA | Distal | 17.182 | 23.841 |
| | Middle | 22.284 | 26.075 |
| | %diff(D: Y-O) | -38.754 | |
| | %diff(M: Y-O) | -17.012 | |
| | %diff(Y: D-M) | -29.693 | |
| | %diff(O: D-M) | -9.372 | |
| S/D-PA | Distal | 14.190 | 20.528 |
| | Middle | 21.770 | 24.388 |
| | %diff(D: Y-O) | -44.669 | |
| | %diff(M: Y-O) | -12.023 | |
| | %diff(Y: D-M) | -53.422 | |
| | %diff(O: D-M) | -18.800 | |
| distal | %diff dd-ss | -0.129 | -60.947 |
| middle | %diff dd-ss | -9.574 | -76.081 |
| distal | %diff ss-dd | 17.414 | 13.893 |
| middle | %diff ss-dd | 2.304 | 6.470 |

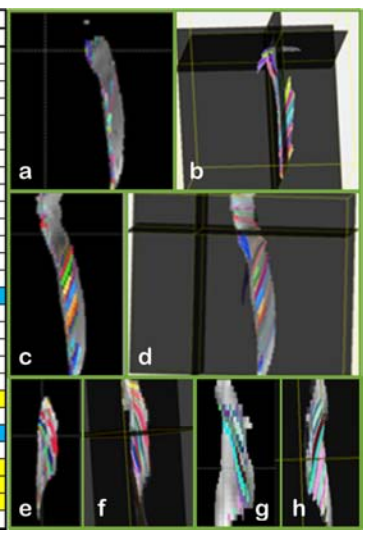


Fig 1: L-R: a: coronal, b: 3D (MG fibers, young subject);
c: coronal, d: 3D (MG fibers, old subject);
e: coronal, f: 3D (LG fibers, young subject);
g: coronal, h: 3D (LG fibers, old subject).
h:3D rotated to show fibers.

**Discussion and Conclusions:** The fiber length changes with age agree with that obtained by ultrasound measurements [1]. The regional dependence of fiber lengths seen here is also anticipated as fibers get shorter as one goes from distal to proximal locations along the muscle. The age related differences in the 'deep' pennation angles agree with earlier findings of a decrease in pennation angle with age. However, in contrast to this, the 'superficial' pennation angles increased with age. The superficial angle can differ from the deep angle either due to fiber curvature or from the relative curvature of the two aponeurosis surfaces. Calculation of the angle of the superficial fiber end with the distal aponeurosis should disambiguate these two situations. From an examination of these values (Table 1), it appears that in the older cohort, fiber curvature contributes to the 'deep' and 'superficial' angle differences while in the younger cohort, the relative curvature of the deep and superficial aponeurosis may contribute to these differences.

**References:** [1] Morse et al. J Appl. Physiol 99, 1050-1055,2005.